# Protein Complexes in the Archaeon *Methanothermobacter thermautotrophicus* Analyzed by Blue Native/SDS-PAGE and Mass Spectrometry*

**Murtada H. Farhoud‡§, Hans J. C. T. Wessels‡§, Peter J. M. Steenbakkers§¶‖, Sandy Mattijssen¶, Ron A. Wevers**, Baziel G. van Engelen‡‡, Mike S. M. Jetten¶, Jan A. Smeitink‡, Lambert P. van den Heuvel‡, and Jan T. Keltjens¶**

***Methanothermobacter thermautotrophicus*** **is a thermophilic archaeon that produces methane as the end product of its primary metabolism. The biochemistry of methane formation has been extensively studied and is catalyzed by individual enzymes and proteins that are organized in protein complexes. Although much is known of the protein complexes involved in methanogenesis, only limited information is available on the associations of proteins involved in other cell processes of *M. thermautotrophicus*. To visualize and identify interacting and individual proteins of *M. thermautotrophicus* on a proteome-wide scale, protein preparations were separated using blue native electrophoresis followed by SDS-PAGE. A total of 361 proteins, corresponding to almost 20% of the predicted proteome, was identified using peptide mass fingerprinting after MALDI-TOF MS. All previously characterized complexes involved in energy generation could be visualized. Furthermore the expression and association of the heterodisulfide reductase and methylviologen-reducing hydrogenase complexes depended on culture conditions. Also homomeric supercomplexes of the ATP synthase stalk subcomplex and the $N^5$-methyl-5,6,7,8-tetrahydromethanopterin:coenzyme M methyltransferase complex were separated. Chemical cross-linking experiments confirmed that the multimerization of both complexes was not experimentally induced. A considerable number of previously uncharacterized protein complexes were reproducibly visualized. These included an exosome-like complex consisting of four exosome core subunits, which associated with a tRNA-intron endonuclease, thereby expanding the constituency of archaeal exosomes. The results presented show the presence of novel complexes and demonstrate the added value of including blue native gel electrophoresis followed by SDS-PAGE in discovering protein complexes that are involved in catabolic, anabolic, and general cell processes.** ***Molecular & Cellular Proteomics 4:1653–1663, 2005.***

*Methanothermobacter thermautotrophicus* is a thermophilic archaeon that generates energy from the reduction of carbon dioxide to methane. In contrast to mostly mesophilic methanogens, *M. thermautotrophicus* can use hydrogen and carbon dioxide only as substrates and is therefore regarded as a metabolic specialist. It has a relatively simple primary metabolism comprising eight consecutive steps (1). Methane production, or methanogenesis, starts with the reduction of carbon dioxide to a formyl moiety that is bound to the C1 carrier methanofuran. The endergonic reaction is catalyzed by a membrane-bound formylmethanofuran dehydrogenase complex and is driven by a gradient of sodium (2). Next the formyl moiety is transferred to a second C1 carrier and reduced by individual, cytosolic enzymes to a methyl moiety. Hereafter the methyl group is transferred to coenzyme M by the membrane-bound $N^5$-methyl-5,6,7,8-tetrahydromethanopterin:coenzyme M methyltransferase complex that simultaneously generates a sodium gradient (3). Finally the methyl group is then reduced to methane by the cytosolic methyl coenzyme M reductase complex (4). Next to methane, the mixed disulfide of coenzyme M and coenzyme B is formed. The heterodisulfide is reduced by the heterodisulfide reductase complex that is supplied with reducing equivalents by the methylviologen-reducing hydrogenase (5). The proton motive force that is generated in this step is finally used by a membrane-bound ATP synthase complex for the production of ATP (6). Next to the generation of ATP, methanogenesis also provides carbon for cell growth through the activity of the acetyl-CoA decarbonylase/synthase complex (7). In natural ecosystems the amount of hydrogen is the limiting substrate for growth and can vary 4 orders of magnitude in availability. As an adapta-

From the ‡Nijmegen Center for Mitochondrial and Metabolic Disorders, Radboud University Nijmegen Medical Center, Geert Grooteplein 10, 6500 HB Nijmegen, ¶Department of Microbiology, Faculty of Science, Radboud University Nijmegen, Toernooiveld 1, 6525 ED Nijmegen, **Department of Pediatrics and Neurology, Radboud University Nijmegen Medical Center, Reinier Postlaan 4, 6525 GC Nijmegen, and ‡‡Neuromuscular Center Nijmegen, Department of Neurology, Radboud University Nijmegen Medical Center, Reinier Postlaan 4, 6525 GC Nijmegen, The Netherlands

Received, June 3, 2005, and in revised form, July 20, 2005

Published, MCP Papers in Press, July 21, 2005, DOI 10.1074/mcp.M500171-MCP200

tion, *M. thermautotrophicus* expresses isoenzymes with a high or low affinity for hydrogen, *e.g.* methyl coenzyme M reductases I and II are expressed under culturing conditions with low and high hydrogen gassing regimes ("MCR[1] I and MCR II culture conditions"), respectively (8).

In a closely related species, *Methanothermobacter marburgensis*, it was shown that complexes of the primary metabolism that are coupled functionally can also interact physically. The purification of heterodisulfide reductase activity resulted in the purification of the heterodisulfide reductase protein complex that also contained the methylviologen-reducing hydrogenase complex (5). In *M. thermautotrophicus*, similarly it was speculated that the association into high molecular weight complexes in concentrated solutions of purified methyl coenzyme M reductase and $F_{420}$-dependent hydrogenase proteins could also play a role *in vivo* (9). Electron microscopy studies of enzymes and complexes involved in methanogenesis of *Methanococcus voltae* and *Methanosarcina mazei* Gö1 showed the associations of methanogenesis enzymes into supercomplexes, named methanoreductosomes (10). These results corroborate the generally accepted idea that the protein content of a cell is not merely a pool of individual and inert proteins but that the proteome of a living cell is an intricate network of proteins that interact and communicate. So far, research on *M. thermautotrophicus* has focused mainly on the enzymes and enzyme complexes that are involved in methanogenesis, and therefore only limited data are available on interacting proteins involved in other cellular processes.

To explore interacting (and non-interacting) proteins of an organism on a proteome-wide scale, only a limited number of techniques are available. One established method is the use of blue native electrophoresis followed by SDS-PAGE (or BN-PAGE) (11). In this method, proteins and protein complexes are solubilized by a mild detergent, charged with Coomassie dye, and separated natively in a first dimension depending on charge, size, and shape. In a second dimension, proteins and protein complexes are reduced and denatured with SDS and subunits, and individual proteins are separated by molecular weight. So far BN-PAGE has been applied mainly to membrane-associated complexes of organelles (12, 13) sometimes after dialysis of protein preparations (11) and often in combination with the use of antibodies.

In this study we present the results of a proteome-wide examination of interacting and individual proteins of *M. thermautotrophicus* using blue native/SDS-PAGE combined with mass spectrometry. This resulted in the identification of 361 proteins, corresponding to almost 20% of the predicted proteome, and visualization of a significant number of proteins that are part of enzyme complexes. These allowed, among others, the identification of an exosome-like complex of *M. thermautotrophicus*. Next to the homologs of four exosome core subunits identified previously (14), the *M. thermautotrophicus* exosome additionally contains a tRNA-intron endonuclease.

In summary, the results presented here give, for the first time, an overview of interacting and individual proteins of the archaeon *M. thermautotrophicus* on a proteome-wide scale using BN-PAGE. The genome coverage and the protein complexes identified by this technique clearly indicate the added value of including BN-PAGE in proteomic research and allow the study of protein complexes involved in primary metabolism, anabolism, and general cell processes.

## EXPERIMENTAL PROCEDURES

*Cultivation and Preparation of Cell-free Extract of M. thermautotrophicus*—*M. thermautotrophicus* (DSM1053) was cultured in a 12-liter fed-batch fermentor containing 10 liters of medium. Cells were cultured under two different conditions, one favoring the expression of MCR I and the other favoring MCR II expression (8). "MCR I" cells were cultured in N medium (15) at 65 °C with a gas flow of 2.0 liters/min of 80% $H_2$, 20% $CO_2$ (v/v) and harvested at an optical density at 600 nm of 5. "MCR II" cells were cultured in MII medium (15) at 55 °C with a gas flow of 5.0 liters/min of 80% $H_2$, 20% $CO_2$ (v/v) and harvested at an optical density at 600 nm of 1.8. After centrifugation, cell-free extracts were prepared by suspending the pellet in 1 volume of 50 mM TES, pH 7.0, 1 mM DTT, including both DNase and RNase at a final concentration of 10 $\mu$g/ml. Cell suspensions were passed through a French pressure cell operated at 138 megapascals. After centrifugation for 15 min at 10,000 $\times$ *g* at 4 °C, the cytosolic fraction was obtained as the clarified supernatant, and the resulting pellet is referred to as the membrane fraction. Both fractions were stored at −20 °C.

*Sample Preparation*—Before protein solubilization, the membrane fraction was washed three times with a solution containing 400 mM sorbitol, 25 mM NaCl, and 7.5 mM imidazole, pH 7.0, to reduce contaminating cytosolic proteins. Cytosolic and membrane protein preparations were diluted with 2–3 volumes of solubilization buffer (50 mM NaCl, 5 mM 6-aminocaproic acid, 1 mM EDTA, and 50 mM imidazole, pH 7.0) containing either 2% (v/v) laurylmaltoside, 1% (v/v) digitonin, or 1% (v/v) Triton X-100. After a 15-min incubation on ice with occasional vortexing samples were centrifuged for 30 min at 12,000 $\times$ *g* at 4 °C. Supernatants were transferred to clean tubes, and protein concentrations were determined with the 2D-Quant kit (Amersham Biosciences). Finally 4 $\mu$l of 750 mM 6-aminohexanoic acid with 5% (w/v) Serva Blue G was added per 100 $\mu$l of supernatant.

*Chemical Cross-linking*—To investigate the association of membrane-bound complexes, the proteins present in the membrane fraction were treated with the 8-Å linker dimethyl 3,3′-dithiopropionimidate dihydrochloride (Sigma) and the "zero-length" carbodiimide cross-linker 1-ethyl-3-(3-dimethylaminopropyl)carbodiimide (EDAC, Molecular Probes) in the presence of *N*-hydroxysulfosuccinimide (NHSS, Molecular Probes) (16). For this, an aliquot of 200 $\mu$l of the membrane fraction of MCR I cells was diluted with 600 $\mu$l of a solution containing 75 mM imidazole, pH 7, 400 mM sorbitol, 25 mM NaCl, and 0.03% laurylmaltoside. The chemical cross-linking reaction was started by adding 40 $\mu$l of freshly prepared 10 mg/ml dimethyl 3,3′-dithiopropionimidate dihydrochloride or 12 $\mu$l each of an 80 mM EDAC and 80 mM NHSS solution and proceeded for 1 h on ice with occa-

[1] The abbreviations used are: MCR, methyl coenzyme M reductase; methyltransferase, $N^5$-methyl-5,6,7,8-tetrahydromethanopterin:coenzyme M methyltransferase; BN-PAGE, blue native gel electrophoresis followed by SDS-PAGE; TES, *N*-Tris(hydroxymethyl)methyl-2-aminoethanesulfonic acid; EDAC, 1-ethyl-3-(3-dimethylaminopropyl)carbodiimide; NHSS, *N*-hydroxysulfosuccinimide; Tricine, *N*-[2-hydroxy-1,1-bis(hydroxymethyl)ethyl]glycine; 2D, two-dimensional.

sional mixing. The reaction was stopped by the addition of ammonium acetate to a final concentration of 0.1 M. As a control, immediately after addition of the cross-linkers, a 200-μl aliquot of the reaction mixture was quenched by adding 50 μl of 0.5 M ammonium acetate. Protein complexes were isolated immediately with either laurylmaltoside or digitonin as described above.

*BN-PAGE and Gel Staining*—Blue native/SDS-PAGE two-dimensional gel electrophoresis was performed as described elsewhere (13, 17, 18) and performed on a Protean II xi system (Bio-Rad). For the blue native first dimension, protein preparations were separated on gels containing the following bis-/acrylamide gradients: 4–13, 5–15, 6–18, 8–20, and 10–22%. The ferritin monomer (440 kDa) and ferritin dimer (880 kDa) were included as markers. Samples were separated overnight at 15 °C at 100 V and typically finished after 16 h.

The second dimension was performed as described elsewhere (19) with some modifications. Individual lanes of the first dimension gel were excised with a razor blade and incubated in 1% (w/v) SDS and 1% (v/v) 2-mercaptoethanol for 1–2 h at room temperature. Next the first dimension lane, which was rinsed with milli-Q to remove excess 2-mercaptoethanol, was placed on top of a separation gel consisting of a 10% Tris-Tricine-SDS gel, which was cross-linked with piperazine diacrylamide. The flanking regions of the first dimension lane were filled with 10% native polyacrylamide gel. Using a notched inner glass plate, the Protean II xi system was converted into a four-gel system and started at a constant current of 5 mA per gel, which was raised to 10 mA after 45 min. Second dimension gels were run overnight at 15 °C and typically finished after 20 h. After the second dimension, gels were stained with colloidal Coomassie as described elsewhere (20) and scanned using an Amersham Biosciences Image Scanner.

*Trypsin Treatment*—After spot picking, protein present in gel plugs was first reduced by incubating for 10 min in 50 μl 10 mM DTT at 60 °C followed by an alkylating incubation of 45 min in 50 μl of 50 mM iodoacetamide at room temperature in the dark. Hereafter in-gel trypsin digestion was performed as described elsewhere (21) except that overnight trypsin treatment was performed in 5 μl of 50 mM ammonium bicarbonate containing 5 mM *n*-octyl glucopyranoside per plug. Next protein fragments were extracted by adding 1 μl of 0.5% (v/v) trifluoroacetic acid, 5 mM *n*-octyl glucopyranoside and incubating for 2 h at room temperature and a final 1-min sonication step. After extraction, peptides were stored at −20 °C until further analysis.

*MALDI-TOF MS Measurements and MASCOT Search Parameters*—For MS analysis, 0.25 μl of extracted peptides was pipetted on a MALDI-TOF sample plate and directly mixed with an equal volume of sample buffer containing 20 mg/ml α-cyano-4-hydroxycinnamic acid in 0.05% (v/v) TFA, 50% (v/v) acetonitrile. MALDI-TOF MS measurements were performed in the mass range of 650–2,600 Da on a Bruker III mass spectrometer, set to reflectron mode, after calibration using a mixture of bradykinin fragment 1–7, angiotensin, synthetic peptide P14R, and adrenocorticotropic hormone fragment 18–39. Mass spectra were determined as the sum of 180 measurements. Monoisotopic peaks were manually selected, excluding background peaks. Peptide masses were exported to Biotools software and used to perform a MASCOT search in an in-house database of the *M. thermautotrophicus* predicted proteome. Search parameters allowed a mass deviation of ±0.3 Da, matching peptides containing one miscleavage, fixed modification of carbamidomethylated cysteines, and a variable modification of oxidized methionines.

*Protein Identification Criteria*—Proteins were regarded as identified proteins when the MASCOT search resulted in a Mowse score higher than 45 (corresponding to an expect score $<10^{-4.5}$), which was calculated from the database size by the MASCOT software. A filter was included to recognize false-positives. A 2D gel electrophoresis study currently in progress has shown that proteins that are identified with matching peptides that mostly contain one miscleavage do not show a correlation between the predicted and experimental location on a 2D gel.[2] Therefore, proteins were only regarded as significantly identified when they showed a Mowse score higher than 45 and contained mostly matching peptides that did not contain a miscleavage. Similar criteria applied for the identification of multiple proteins in a single spot. Here proteins were regarded as identified when peptides unique to that protein matched the above mentioned criteria.

*LC-MS/MS Measurements and Protein Identification Procedure*—All nanoflow LC-MS/MS experiments were performed on a 7-tesla Finnigan LTQ-FT mass spectrometer (Thermo Electron) equipped with a nanoelectrospray ion source (Proxeon Biosystems, Odense, Denmark). The LC part of the analytical system consisted of an Agilent Series 1100 nanoflow LC system (Waldbronn, Germany) comprising a solvent degasser, a nanoflow pump, and a thermostated microautosampler. Chromatographic separation of the peptides was performed in a 15-cm fused silica emitter (100-μm inner diameter; New Objective) packed in-house with methanol slurry of reverse-phase ReproSil-Pur $C_{18}$-AQ 3-μm resin (Dr. Maisch GmbH, Ammerbuch-Entringen, Germany) at a constant pressure (20 bars) of helium. Then 5 μl of the tryptic peptide mixtures were autosampled onto the packed emitter with a flow of 600 nl/min for 20 min and then eluted with a 5-min gradient from 3 to 10% followed by a 25-min gradient from 10 to 30% acetonitrile in 0.5% acetic acid at a constant flow of 300 nl/min. The mass spectrometer was operated in the data-dependent mode to automatically switch between MS and MS/MS acquisition. Survey MS spectra (from *m/z* 350 to 2,000) were acquired in the FTICR with $r = 50{,}000$ at *m/z* 400 (after accumulation to a target value of 1,000,000). The three most intense ions were sequentially isolated for fragmentation in the linear ion trap using collisionally induced dissociation with normalized collision energy of 29% and a target value of 1,000. Former target ions selected for MS/MS were dynamically excluded for 30 s. Total cycle time was ~3 s.

Proteins were identified via automated database searching (Matrix Science, London, UK) of all tandem mass spectra against both NCBInr and an in-house curated *M. thermautotrophicus* database. Carbamidomethylcysteine was set as fixed modification, and oxidized methionine and protein *N*-acetylation were searched as variable modifications. Initial mass tolerances for protein identification on MS and MS/MS peaks were 10 ppm and 0.5 Da, respectively. The instrument setting for the MASCOT search was specified as "ESI-Trap."

*Protein Annotation and Similarities and Genomic Organization of Encoding Genes*—The proteins identified were annotated on basis of the presence of domain signatures of the Pfam database (22). Sequence similarities were determined using Blast 2 sequences (23) at default settings. The organization of genes into operons was determined from the gene organization at the PEDANT website (24). Genes were considered to be part of an operon when the intergenic distance was smaller than 55 bp.

## RESULTS

The proteome of *M. thermautotrophicus* was analyzed using BN-PAGE to investigate the presence of enzyme complexes and individual enzymes. Biomass was collected after culturing under MCR I or MCR II conditions (see "Experimental Procedures"). For both culture conditions, lysed cells were separated into a cytosolic and a membrane fraction by cen-

[2] M. H. Farhoud, J. C. T. Wessels, P. J. M. Steenbakkers, W. Pluk, E. Lasonder, I. Schmidt, R. A. Wevers, B. G. van Engelen, M. S. M. Jetten, J. A. Smeitink, L. P. van den Heuvel, and J. T. Keltjens, unpublished data.

trifugation to reduce the complexity of the sample. The protein preparations were subjected to blue native gel electrophoresis directly without any additional cleaning procedures.

Different first dimension gradients were applied to achieve maximum resolution of individual and complexed proteins. Typically individual proteins were optimally resolved with a first dimension gradient running from 10 to 20% bis-/acrylamide, whereas protein complexes showed maximum resolution with gradients starting at 4% bis-/acrylamide. Next to an optimization of the electrophoresis procedure and protein load, the identification of proteins also was optimized. The use of colloidal Coomassie staining in comparison to silver staining or traditional Coomassie staining enabled a high sensitivity while remaining completely compatible with mass spectrometry. Another improvement was the alkylation of cysteine residues after spot picking, which greatly reduced the number of background peaks after MALDI-TOF MS measurements and allowed the identification of multiple proteins in a single spot. An initial analysis of protein spots from duplicate gels and duplicate biological samples confirmed the reproducibility of BN-PAGE.

*Identification of Proteins after BN-PAGE*—The complete data set comprised the analysis of 1,550 protein spots by peptide mass fingerprinting. The data set included the optimization procedures, the appropriate reference protein spots from duplicate gels, and the identification of putative complex components originating from multiple blue native gels with different bis-/acrylamide gradients. The analysis showed that only a minor portion of the proteins identified appeared at multiple positions on gels and that no detectable protein degradation had taken place. The analysis of ~875 protein spots of the proteins extracted from the membrane fraction allowed the identification of 300 different proteins, whereas the analysis of 675 protein spots from the cytosolic fraction identified 223 proteins. A total of 361 different proteins (for a reference map see Supplemental Fig. 1) were identified with an average Mowse score of 122 (which corresponds to an expect value less than $10^{-12}$) and an average protein sequence coverage of 37% (see Supplemental Table 1). Five percent of the predicted membrane proteins (34 of 407 proteins containing one or more predicted transmembrane-spanning regions) were retrieved. This was also reflected in the coverages of the different protein function categories that were recognized after initial analyses of the *M. thermautotrophicus* genome (25). A relatively low coverage of proteins involved in transport or in membrane and cell wall synthesis was apparent. In contrast to the results for hydrophobic proteins, 22% of the total number of cytoplasmic proteins was recovered. These 327 proteins distributed more or less equally along the different protein function categories, and all of the previously characterized methanogenesis enzymes were identified. However, only a small number of hypothetical and conserved hypothetical proteins were recovered (34 proteins identified of 538 predicted). A higher coverage was obtained for enzymes involved in primary metabolism, amino acid metabolism, and other anabolic processes and included a relatively high coverage of ribosomal proteins (31 proteins identified of 63 predicted) and aminoacyl-tRNA synthetases (22 proteins identified of 26 predicted).

*Identification of Homomeric Protein Complexes*—A considerable amount of protein migrated as protein complexes. To identify true protein complexes, different first dimension gradients were applied to track complexes and to exclude any accidental co-migration of proteins. This was, however, limited to complexes that were resolved by gradients starting at 4% bis-/acrylamide or higher and not for complexes migrating at an extremely high apparent molecular mass (>1.5 MDa). A number of homomeric complexes were identified that were isolated previously from *M. thermautotrophicus*. Coenzyme $F_{420}$-dependent $N^5$,$N^{10}$-methylene tetrahydromethanopterin dehydrogenase migrated as a 200-kDa complex, corresponding with the molecular mass of 216 kDa of the hexameric complex as determined earlier (26). The most prominent protein present in cell-free extracts of *M. thermautotrophicus*, MTH1350,[3] a $F_{420}$-dependent oxygen detoxification flavoprotein, was purified previously as a 170-kDa homotetrameric complex (27). Here the protein complex could be clearly visualized migrating at an apparent molecular mass of 150 kDa. Next to the previously characterized complexes, a number of uncharacterized, putative homomeric complexes were recognized. These included an 800-kDa complex of the 15-kDa riboflavin synthase MTH1390 indicating an organization of this enzyme into a 50-mer, which is consistent with earlier reports (28, 29). A 700-kDa complex of the 73-kDa protein MTH632 containing a putative sugar kinase domain was identified, suggesting a decameric organization. A 300-kDa complex was identified for the 28-kDa MTH579 fructose-1,6-bisphosphate aldolase, suggesting an 8–12 multimeric organization of this protein (30). Similarly porphobilinogen synthase, MTH744, migrated as a complex of 300 kDa. This value corresponds with a homooctamer, and this quaternary organization is known to be intrinsic to the allosteric regulatory mechanism of these enzymes (31). A putative dimer and trimer migrating at 100 kDa were found, respectively, for MTH1476 encoding a homolog of the $\beta$ subunit of the tryptophan synthase and MTH1512 encoding a homolog of the $H_2$-dependent $N^5$,$N^{10}$-methylenetetrahydromethanopterin dehydrogenase (Table I).

Although the quaternary structures determined by BN-PAGE correspond well to values reported for homologs purified from other hosts, it should be noted that BN-PAGE cannot discriminate between monomeric enzymes and homomeric complexes. Proteins that migrate poorly in the first dimension (because of an extreme amino acid composition or protein shape) and enzyme complexes that are composed of a single

[3] MTH and number refers to the open reading frame number of the *M. thermautotrophicus* genome.

TABLE I
*Homomeric complexes from M. thermautotrophicus*

Complexes are listed by MTH number. The complexes identified are given with the calculated molecular mass of the subunit, the Mowse score, sequence coverage (%), the observed and reported molecular masses of the complexes, and the derived number of subunits. Molecular masses are given in kDa.

| MTH | Annotation | Calculated molecular mass of subunit | Mowse score | Sequence coverage | Observed molecular mass | Reported molecular mass (Ref.) | No. of subunits |
|---|---|---|---|---|---|---|---|
| 579 | Fructose-1,6-bisphosphate aldolase | 28 | 123 | 46 | 300 | | 10 |
| 632 | Putative phosphofructo- (sugar) kinase | 72.7 | 260 | 46 | 700 | | 10 |
| 744 | Porphobilinogen synthase | 35.8 | 140 | 48 | 300 | | 8 |
| 1350 | Flavoprotein AI | 46 | 210 | 44 | 150 | 170 (27) | 4 |
| 1390 | Riboflavin synthase $\beta$ subunit | 15.5 | 91 | 56 | 800 | | 50 |
| 1464 | $F_{420}$-dependent $N^5$,$N^{10}$-methylene tetrahydromethanopterin dehydrogenase | 29.6 | 121 | 40 | 200 | 200 (26) | 6 |
| 1476 | Tryptophan synthase, $\beta$ subunit homolog | 47.5 | 215 | 57 | 100 | | 2 |
| 1512 | $H_2$-dependent $N^5$,$N^{10}$-methylenetetrahydro-methanopterin dehydrogenase homolog | 37.3 | 82 | 27 | 100 | | 3 |

subunit species can, theoretically, migrate equal distances in blue native gels. This can be excluded for complexes consisting of different subunits. Next to the homomeric complexes mentioned, a considerable number of heteromeric complexes were identified that can be divided roughly into complexes involved in energy generation and those involved in anabolic and general cell processes.

*Heteromeric Complexes Involved in Energy Generation*—To evaluate BN-PAGE as a mild technique that can be used to identify protein associations, specific attention was given to the analysis of protein complexes involved in methanogenesis. Because of the extensive biochemical research that has been performed on methanogenesis, these complexes were regarded as internal standards. The use of BN-PAGE followed by mass spectrometry visualized and identified all enzyme complexes involved in methanogenesis (Table II).

One of the most dominant complexes present in both cytosolic as well as membrane fractions were the MCR complexes I and II, migrating at an apparent molecular mass of 250 kDa (4). Both MCR complexes contained the highly similar $\alpha$, $\beta$, and $\gamma$ subunits in apparently equal amounts as was judged from their relative staining intensities. In agreement with literature, protein preparations derived from cells grown under MCR I conditions predominantly contained the subunits from the MCR I complex, whereas protein from MCR II culturing conditions contained the MCR II subunits (8). Also experimental evidence was found in the cytosolic fraction for the catalytic portion of the tungsten-dependent formylmethanofuran dehydrogenase complex. It migrated at an apparent molecular mass of ~100 kDa and contained the subunits A, B, and D (32–34). The subunits of the $N^5$-methyl-5,6,7,8-tetrahydromethanopterin:coenzyme M methyltransferase (methyltransferase) were predominantly present in the membrane protein fraction and migrated as a complex composed of subunits A, C, D, E, F, G, and H with an apparent molecular mass of 900 kDa (3). The heterodisulfide reductase complex was detected predominantly in the cytosolic fraction and appeared as two separate complexes of ~300 and 400 kDa, respectively. Both complexes contained the three subunits A, B, and C. The heterodisulfide reductase complex migrating at the highest apparent molecular mass further showed the presence of methylviologen-reducing hydrogenase subunits $\alpha$, $\gamma$, and $\delta$, which were also detected in a separate complex migrating at ~100 kDa (35). The heterodisulfide reductase complex migrating at the highest apparent molecular mass represented an association of the heterodisulfide reductase complex with the methylviologen-reducing hydrogenase complex. Interestingly the relative amount of individual heterodisulfide reductase complex and heterodisulfide reductase complex associated with the methylviologen-reducing hydrogenase differed in cytoplasmic protein preparations obtained from cells grown under MCR I and MCR II culture conditions. As estimated from the relative staining intensities, cells cultured at MCR I conditions contained at least 3-fold more of the individual heterodisulfide reductase complex and the same complex associated with the methylviologen-reducing hydrogenase than cells cultured under MCR II conditions (Fig. 1).

In contrast to the methylviologen-reducing hydrogenase, the coenzyme $F_{420}$-reducing hydrogenase complex was found exclusively as a separate, high molecular weight complex. It migrated with an apparent molecular mass of ~900 kDa, corresponding with the previously reported mass of 800 kDa (36), and consisted of three protein spots. The protein spots of 45, 30, and 25 kDa corresponded to subunits $\alpha$, $\beta$, and $\gamma$, respectively. Despite a considerable amount of protein, the $\gamma$ subunit could not be identified by peptide mass fingerprinting and was identified unambiguously by LC-MS/MS.

Next to the methanogenesis complexes (Table II), the archaeal ATP synthase was exclusively visualized in the membrane fraction by BN-PAGE. ATP synthase migrated as two separate subcomplexes containing either the membrane (A0) or catalytic part (A1) of the ATP synthase complex. Four

TABLE II

*Overview of heteromeric complexes in M. thermautotrophicus*

Complexes are listed in the order of appearance in the text. The complexes are given with the Mowse score and sequence coverage (%) of the subunits identified, the calculated molecular masses of the subunits, and the observed and reported molecular masses of the complexes in kDa.

| MTH | Annotation | Mowse score | Sequence coverage | Molecular mass of subunit | Complex molecular mass | Reported molecular mass (Ref.) |
|---|---|---|---|---|---|---|
| | Methyl coenzyme M reductase I | | | | 250 | 275 (4) |
| 1164 | α subunit | 209 | 39 | 60.5 | | |
| 1165 | γ subunit | 156 | 45 | 29.1 | | |
| 1168 | β subunit | 177 | 42 | 48.1 | | |
| | Methyl coenzyme M reductase II | | | | 250 | 275 (4) |
| 1129 | α subunit | 178 | 33 | 60.7 | | |
| 1130 | γ subunit | 303 | 73 | 30.6 | | |
| 1132 | β subunit | 103 | 34 | 47.5 | | |
| | Tungsten-dependent formylmethanofuran dehydrogenase | | | | 100 | 130 (32) |
| 1557 | Subunit A | 101 | 24 | 62.9 | | |
| 1558 | Subunit C | 124 | 54 | 28.6 | | |
| 1559 | Subunit B | 137 | 49 | 48.9 | | |
| | Methyltransferase | | | | 900 | 670 (3) |
| 1156 | Subunit H | 160 | 58 | 33.4 | | |
| 1157 | Subunit G | 113 | 58 | 9.5 | | |
| 1158 | Subunit F | 77 | 51 | 7.4 | | |
| 1159 | Subunit A | 63 | 38 | 25.66 | | |
| 1161 | Subunit C | 58 | 16 | 27.0 | | |
| 1162[a] | Subunit D | 45 | 5 | 22.8 | | |
| 1163[a] | Subunit E | 128 | 17 | 31.2 | | |
| | Heterodisulfide reductase | | | | 300/400 | 250/500 |
| 1381 | Subunit A | 210 | 43 | 73.5 | | (5) |
| 1878 | Subunit C | 106 | 31 | 36.0 | | |
| 1879 | Subunit B | 96 | 34 | 33.5 | | |
| | Methylviologen-reducing hydrogenase | | | | 100/400 | 500 |
| 1134 | α subunit | 233 | 38 | 52.9 | | (5) |
| 1135 | γ subunit | 54 | 23 | 33.8 | | |
| 1136 | δ subunit | 89 | 46 | 15.9 | | |
| | $F_{420}$-reducing hydrogenase | | | | 1,000 | 800 (37) |
| 1297 | β subunit | 103 | 34 | 30.8 | | |
| 1298[a] | γ subunit | 120 | 14 | 25.8 | | |
| 1300 | α subunit | 164 | 33 | 45.2 | | |
| | A1 subcomplex ATP synthase | | | | 400 | |
| 953 | Subunit D | 173 | 71 | 24.5 | | |
| 954 | Subunit B | 248 | 44 | 51.9 | | |
| 955 | Subunit A | 316 | 55 | 64.9 | | |
| 956 | Subunit F | 75 | 51 | 11.8 | | |
| | A0 subcomplex ATP synthase | | | | 600 | |
| 957 | Subunit C (γ) | 105 | 34 | 42.4 | | |
| 958 | Subunit E (ε) | 163 | 73 | 22.7 | | |
| 960 | Subunit I | 266 | 34 | 74.5 | | |
| 961[a] | Subunit H | 109 | 20 | 11.8 | | |
| | Acetyl-CoA decarbonylase/synthase | | | | 1,200 | |
| 1708 | α subunit | 69 | 14 | 86.1 | | |
| 1710 | β subunit | 144 | 30 | 51.7 | | |
| 1713 | γ subunit | 77 | 33 | 50.2 | | |
| | Lipid biosynthesis precursor | | | | 300 | |
| 792 | 3-Hydroxy-3-methylglutaryl-CoA synthase | 127 | 27 | 37.1 | | |
| 793 | Acetoacetyl-CoA thiolase | 144 | 44 | 40.5 | | |
| | Phenylalanine-tRNA synthetase | | | | 300 | |
| 742 | α subunit | 273 | 45 | 58.5 | | |
| 770 | β subunit | 138 | 22 | 69.4 | | |
| | Fe-S cluster assembly complex | | | | 200 | |
| 1149 | Ycf16 (homolog SufC) | 110 | 48 | 27.7 | | |

TABLE II—*continued*

| MTH | Annotation | Mowse score | Sequence coverage | Molecular mass of subunit | Complex molecular mass | Reported molecular mass (Ref.) |
|---|---|---|---|---|---|---|
| 1150 | Ycf24 (homolog SufB) | 176 | 40 | 45.3 | | |
| | Proteasome | | | | 800 | |
| 686 | $\alpha$ subunit | 184 | 54 | 27.5 | | |
| 1202 | $\beta$ subunit | 129 | 58 | 22.8 | | |
| | Proteasome regulator | | | | 800 | |
| 540 | Rad50 ATPase | 246 | 29 | 97.6 | | |
| 728 | Proteasome-activating nucleotidase | 205 | 32 | 46.1 | | |
| | Exosome | | | | 900 | |
| 682 | RNA exonuclease (Rrp42) | 90 | 22 | 29.9 | | |
| 683 | Ribonuclease PH (Rrp41) | 149 | 51 | 26.5 | | |
| 684 | Conserved protein (Rrp4) | 94 | 28 | 34.7 | | |
| 891 | DnaG homolog | 136 | 31 | 42.5 | | |
| 250 | tRNA-intron endonuclease | 56 | 35 | 19.7 | | |

[a] Identified by LC-MS/MS.

protein bands corresponding to the A1 ATP synthase subunits A, B, D, and F migrated as one complex of 400 kDa. The membrane-embedded part or A0 segment of the ATP synthase migrated at a higher apparent molecular mass of 600 kDa and also contained four protein bands, which were identified as ATP synthase subunits C, E, H, and I. In contrast to the subunit topology determined for the *Methanococcus jannaschii* A0 and A1 ATP synthase subcomplexes, subunit C was only found in the A0 segment (6).

*Supercomplexes*—Interestingly A0 ATP synthase subunits I, C, and H were also identified migrating at 800 kDa and 1 MDa as multimers of the proton-translocating segment of the ATP synthase subcomplex (Fig. 2*A*).

To further investigate the presence of supercomplexes in the cytosolic and membrane fractions, proteins were solubilized using digitonin, which maintains weak protein-protein interactions that are normally disrupted by laurylmaltoside. The laurylmaltoside- and digitonin-treated proteins were essentially identical, and no significant differences could be observed for cytosolic proteins. However, a pronounced difference in the apparent high molecular mass region could be observed when digitonin was used to solubilize membrane proteins. Although no complete ATP synthase complex was solubilized by digitonin, three forms of the A0 subcomplex of the ATP synthase at 600, 800, and 1,000 kDa were apparent that all contained the A0 ATP synthase subunit H (Fig. 2*B*). The E subunit, which overlapped with the subunit H of the methyltransferase complex, was also identified unambiguously in these gels using LC-MS/MS. The sodium-translocating methyltransferase complex appeared as a single complex of 900 kDa in laurylmaltoside-extracted preparations and migrated partly as a multimer of identical composition in digitonin-extracted preparations. To exclude multimerization of both complexes as an experimental artifact, the migration of both complexes was investigated after chemical cross-linking using a zero-length (Fig. 2*C*) and an 8-Å linker chemical cross-linker (data not shown). These experiments showed that cross-linked proteins extracted with laurylmaltoside contained monomers as well as multimers of the complexes mentioned, consistent with the complexes visualized after digitonin extraction. Therefore, the appearance of both ion-translocating complexes as multimers seems to be an intrinsic characteristic of both complexes and is not the result of an experimentally induced, aspecific interaction. Furthermore the chemical cross-linking experiments resulted in the appearance of a complex of 1.2 MDa containing both A0 ATP synthase subunits and methyltransferase subunits, which could reflect a supercomplex of these ion-translocating complexes, that is normally disrupted by solubilization with either laurylmaltoside or digitonin (Fig. 2*C*). However, it cannot be excluded that both multimeric forms co-migrate at this high apparent molecular weight.

*Heteromeric Complexes Involved in Anabolic Processes*—Next to enzyme complexes involved in catabolism, complexes that are involved in biosynthesis also were identified. A complex that migrated with an apparent molecular mass higher than 1.5 MDa, which could just be resolved with a bis-/acrylamide gradient starting at 4% in the first dimension, was the core of the acetyl-CoA decarbonylase/synthase complex (7). It contained the subunits $\alpha$, $\beta$, and $\gamma$ subunits (MTH1708, MTH1710, and MTH1713, respectively). The acetyl-CoA decarbonylase/synthase complex migrated with two proteins predicted to be involved in DNA repair and protein synthesis. Probably the observed associations of the proteins mentioned with the acetyl-CoA decarbonylase/synthase complex is due to the low resolving power at these extremely high apparent molecular weights.

Next to a complex involved in acetyl-CoA synthesis also a putative acetyl-CoA-converting complex was identified. The complex was composed of two proteins, MTH792 and MTH793, of which the encoding genes also constitute an operon. Both proteins appeared in a 1:1 ratio as was judged from their respective staining intensities. The MTH792 and MTH793 proteins are annotated as a 37-kDa 3-hydroxy-3-

methylglutaryl-CoA synthase and a 40-kDa acetoacetyl-CoA thiolase, respectively, that consecutively would convert acetyl-CoA to 3-hydroxy-3-methylglutaryl-CoA, a precursor for lipid biosynthesis. The apparent molecular mass of 300 kDa of the complex suggests that it is composed of a tetramer of both subunits. Although this protein association has not been observed earlier, in radish seedlings, both activities are located in a single polypeptide (37).

Also MTH742 and MTH770 were found as a 300-kDa complex comprising the phenylalanine-tRNA synthetase $\alpha$ and $\beta$ subunits, respectively. MTH1501 represents an additional copy on the genome of the $\alpha$ chain, which was not found associated with MTH770, suggesting that MTH742 is the true phenylalanine-tRNA synthetase $\alpha$ subunit in the preparations tested.

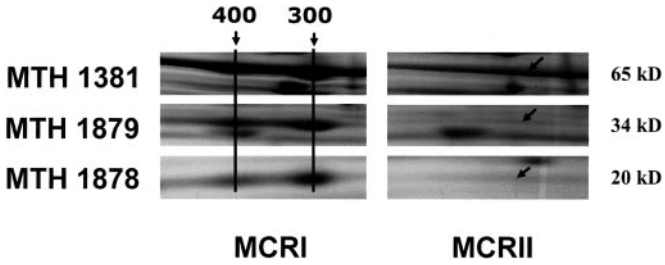


FIG. 1. **The expression and association of the heterodisulfide reductase complex with methylviologen hydrogenase is regulated by culture conditions.** Protein samples were prepared as described under "Experimental Procedures," and 500 $\mu$g of cytosolic protein from cells cultured under MCR I and MCR II conditions were analyzed on 5–15% blue native gels in the first dimension (depicted *horizontally*) and 10% Tris-Tricine-SDS gels in the second dimension (depicted *vertically*). The gels were stained with colloidal Coomassie. The expected positions of heterodisulfide reductase subunits in the MCR II protein preparation are indicated with *arrows*. The apparent molecular masses of the individual and associated heterodisulfide reductase complexes are given in kDa. The subunits of the methylviologen hydrogenase are not shown.

The 28-kDa MTH1149 and 45-kDa MTH1150 annotated as ATP-binding cassette transporter subunits Ycf16 and Ycf24 formed a complex of 200 kDa in a 1:1 ratio. Both encoding genes constitute an operon and encode two homologs of the iron uptake system, SufC and SufB, of *Escherichia coli* (56 and 41% sequence similarity, respectively) and *Thermotoga maritima* (61 and 48% sequence similarity, respectively). These proteins are involved in the protection of iron-sulfur clusters of proteins under oxidative stress conditions (38, 39) and have been shown to interact but so far not in Archaea.

*Heteromeric Complexes Involved in General Processes*—Complexes also were identified that are involved in general cell processes of *M. thermautotrophicus*, *i.e.* the proteasome and exosome involved in protein and RNA processing, respectively (40). A clearly visible complex was formed by the $\alpha$ and $\beta$ subunits of the proteasome, MTH686 and MTH1202, respectively, migrating at an apparent molecular mass of 800 kDa (41). Interestingly the proteasome-activating nucleotidase protein MTH728 (42) was found in the same mass range as the proteasome but was not associated with the proteasome subunits (43, 44). MTH728 migrated as an 800-kDa complex with MTH540 in a 1:1 ratio. Although the MTH540 protein is annotated as a homolog of the Rad50 protein involved in DNA repair, the Rad50 signature was not recognized at the Pfam website in the MTH540 protein sequence and

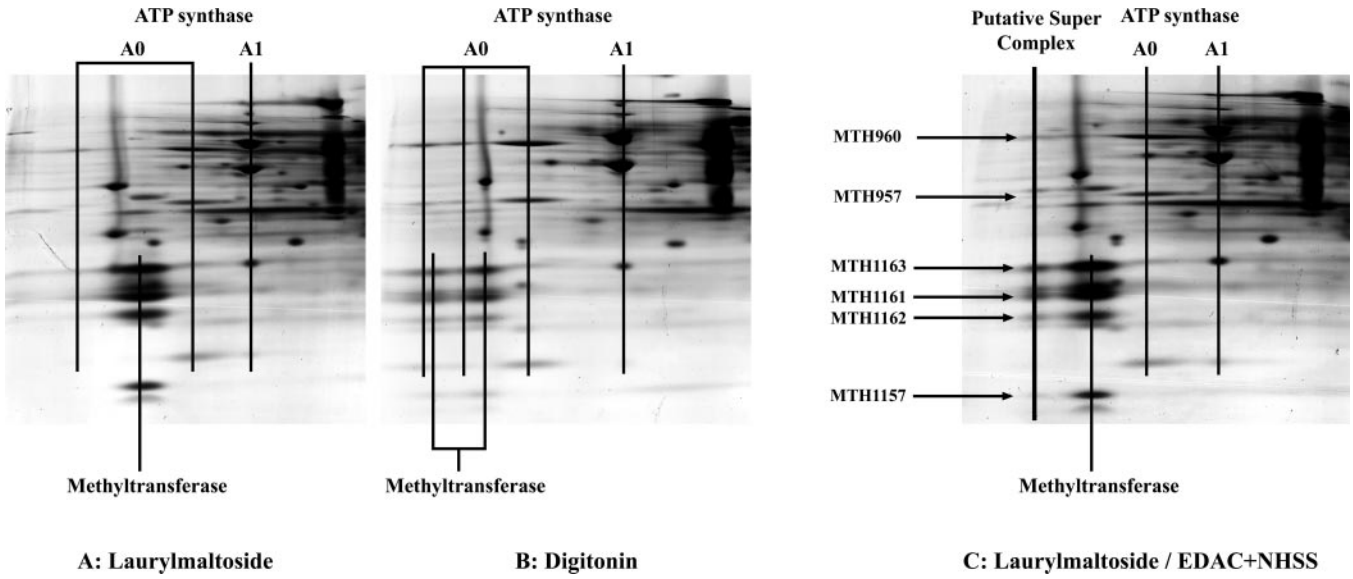


FIG. 2. **The A0 ATP synthase subcomplex and methyltransferase complex form multimers.** The membrane fraction of MCR I cultured cells was solubilized with laurylmaltoside (*A*), digitonin (*B*), or laurylmaltoside after cross-linking with EDAC in the presence of NHSS (*C*) as described under "Experimental Procedures." Five hundred micrograms of protein from each incubation were analyzed on 5–15% blue native gels in the first dimension (depicted *horizontally*) and 10% Tris-Tricine-SDS gels in the second dimension (depicted *vertically*). Gels were stained with colloidal Coomassie. Complexes are indicated with *black*, *vertical lines*. The proteins present in the putative supercomplex are given with their respective MTH *numbers*.

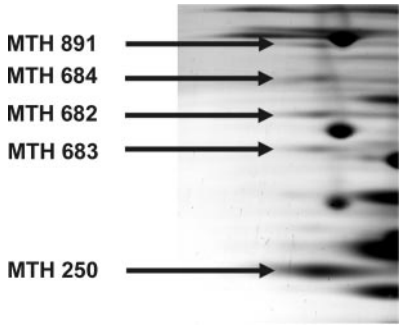


FIG. 3. **The exosome-like complex of *M. thermautotrophicus*.** The cytosolic fraction of cells cultured under MCR I conditions was solubilized with laurylmaltoside as described under "Experimental Procedures." Five hundred micrograms of protein was analyzed on a 5–15% blue native gel in the first dimension (depicted *horizontally*) and a 10% Tris-Tricine-SDS gel in the second dimension (depicted *vertically*) and stained with colloidal Coomassie. The constituents of the exosome-like complex are indicated with their respective MTH *numbers*.

therefore is unlikely to be the homolog of the Rad50 protein in *M. thermautotrophicus*. Next to the proteasome complex and its regulatory protein, also the RNA-processing exosome complex was visualized at 900 kDa. In higher eukaryotes, this complex is involved in the processing of coding and non-coding RNA (45). The *M. thermautotrophicus* exosome complex consisted of four subunits corresponding to MTH682, MTH683, MTH684, and MTH891, which are the orthologs of the core subunits recognized previously in the *Sulfolobus solfataricus* exosome: Rrp42 (63% sequence similarity), Rrp41 (72% sequence similarity), Rrp4 (55% sequence similarity), and DnaG (68% sequence similarity), respectively (14). In analogy with the *S. solfataricus* exosome, the four core subunits appeared with similar staining intensities and were identical to the exosome preparation from *S. solfataricus* after immunoprecipitation of an anion-exchange column-enriched protein preparation (Fig. 3).

No evidence was found for the presence of the Cdc48, yeast Csl4, and chaperonin homologs that were identified in the exosome preparation of *S. solfataricus* immunoprecipitated from crude protein preparations (14). Additionally a protein associated with the *M. thermautotrophicus* exosome with a significantly higher staining intensity relative to the core subunits in cytosolic protein from MCR I cells was found (Fig. 3). This exosome-associated protein was identified as MTH250 encoding the tRNA-intron endonuclease (46). A possible explanation for the great differences in staining intensities might be that the *M. thermautotrophicus* exosome contains the four core subunits mentioned and associates with homomeric complexes of the tRNA-intron endonuclease subunits. This was corroborated by the relative staining intensities of the exosome subunits in cytosolic protein from MCR II cells. Here again the exosome core subunits had identical staining intensities, whereas the intron endonuclease was less prominently present (results not shown). Furthermore the association of the intron endonuclease as a separate complex with the exosome is consistent with the observation of the heterologous tRNA-intron endonuclease isolated from the closely related methanogen *Methanococcus jannaschii* associating spontaneously into homomeric tetramers (46). In conclusion, the composition of the exosome revealed by BN-PAGE shows that, next to the core exosome subunits, the *M. thermautotrophicus* exosome contains or associates with previously unknown RNA processing activities, *i.e.* the intron endonuclease.

## DISCUSSION

The phenotype of microorganisms is the result of the biochemical reactions and responses of the enzymes excreted in the medium and those present in the cytoplasm, membrane, and proteins associated with the cell wall. It is generally accepted that the enzymes and proteins are not merely inert, independent functional units but that proteins interact and in this way form an intricate network, enabling microorganisms to sense their environment and to translate environmental triggers into an adaptation of their enzyme content.

Currently many techniques are used to study the protein content of organisms on a proteome-wide scale and to study the change of the proteome constituency depending on the environmental conditions applied. However, only a limited number of techniques are available to visualize and identify the interaction of proteins *in vivo* and on a proteome-wide scale. One established method of visualizing protein-protein interactions is the use of BN-PAGE (13). To date, this method is used to study specific complexes in combination with antibodies to identify proteins and to prove the multimeric nature of the protein complex under investigation (11).

*Evaluating BN-PAGE as a Tool in Proteomics*—In the study presented here we explored the use of BN-PAGE combined with mass spectrometry to visualize and identify interacting and individual proteins of *M. thermautotrophicus* on a proteome-wide scale. The obtained results show that BN-PAGE can compete with published proteome studies using traditional 2D gel electrophoresis and in fact surpasses the genome coverages obtained in most cases. Despite a relatively high coverage of predicted cytoplasmic proteins, parallel to traditional 2D gel electrophoresis (47), a low coverage was found for proteins containing one or more predicted transmembrane-spanning regions.

To visualize protein-protein interactions, the enzyme complexes involved in methanogenesis were used as internal standards because of the extensive biochemical research that has been performed on these enzyme complexes. All of the previously characterized protein complexes involved in the primary metabolism of *M. thermautotrophicus* were identified, indicating the mild nature of the method used, and furthermore showed that different bis-/acrylamide gradients in the first dimension could be used to exclude any accidental co-migration of proteins and as such identify members of uncharacterized complexes.

*Supercomplexes*—The association of complexes involved in methanogenesis that was observed earlier in *M. marburgensis* (5) also was reproduced by BN-PAGE. The heterodisulfide reductase complex was found as a separate complex and associated partly with the methylviologen-reducing hydrogenase complex under MCR I culture conditions. A comparison of the protein preparations obtained from cells cultured under MCR I and MCR II conditions with regard to the individual and associated forms of the heterodisulfide reductase complex showed considerable differences. Under MCR I conditions a considerable amount of the individual heterodisulfide reductase and the supercomplex were present that were hardly detectable under MCR II conditions. Apparently MCR I conditions induced heterodisulfide reductase and methylviologen hydrogenase components and furthermore triggered a physical link between these two complexes. One possible explanation might be that the amount and the association of both complexes of which one consumes reducing equivalents and the other complex supplies reducing equivalents would ensure that the reaction proceeded under low hydrogen (MCR I) conditions. These results furthermore suggest that, next to a regulation at the expression level, the association of complexes also might be part of the adaptations of the primary metabolism to a change in substrate supply.

"Homomeric" supercomplexes could be recognized for the membrane-associated methyltransferase complex and the ATP synthase stalk subcomplexes, respectively. The observation that ATP synthase complexes form multimers has only been observed for ATP synthases isolated from mitochondria (18) and chloroplasts (48) but not for bacterial ATP synthases (49). The multimerization of the *M. thermautotrophicus* ATP synthase subcomplex is therefore a unique observation for bacterial ATP synthases. However, to determine the exact function of the multimerization of the ATP synthase or the methyltransferase complex more research is required.

The present study has shown the ability of BN-PAGE to reproducibly separate individual proteins and reveal protein-protein interactions, consistent with the results obtained after independent, traditional purification procedures. Next to the identification of a considerable fraction of the predicted proteome, BN-PAGE can visualize the complexes involved in primary metabolism and in anabolic and general processes. Moreover BN-PAGE enables the comparison of the association of complexes between protein preparations obtained from cells cultured under different conditions. As such, BN-PAGE contributes considerably to the knowledge of the protein-protein interactions taking place and to the exact constituency of complexes that are involved in the major cell processes.

*Acknowledgments*—We thank Huub Op den Camp, John Hermans, Wim Geerts, and Leo Nijtmans for discussions and technical assistance.

* Part of this work was supported by the Sixth Framework Program Priority 1, project titled "Rational treatment strategies combating mitochondrial oxidative phosphorylation (OXPHOS) disorders (Eumitocombat), Contract Number 503116. The costs of publication of this article were defrayed in part by the payment of page charges. This article must therefore be hereby marked "*advertisement*" in accordance with 18 U.S.C. Section 1734 solely to indicate this fact.

S The on-line version of this article (available at http://www.mcponline.org) contains supplemental material.

§ These authors contributed equally to this work.

‖ To whom correspondence should be addressed: Dept. of Microbiology, Faculty of Science, Radboud University Nijmegen, Toernooiveld 1, 6525 ED Nijmegen, The Netherlands. Tel.: 31-24-3652568; Fax: 31-24-3652830; E-mail: P.Steenbakkers@science.ru.nl.

REFERENCES

1. Deppenmeier, U. (2002) The unique biochemistry of methanogenesis. *Prog. Nucleic Acids Res. Mol. Biol.* **71,** 223–283
2. de Poorter, L. M. I., Geerts, W. G., Theuvenet, A. P. R., and Keltjens, J. T. (2003) Bioenergetics of the formyl-methanofuran dehydrogenase and heterodisulfide reductase reactions in *Methanothermobacter thermautotrophicus*. *Eur. J. Biochem.* **270,** 66–75
3. Gartner, P., Ecker, A., Fischer, R., Linder, D., Fuchs, G., and Thauer, R. K. (1993) Purification and properties of $N^5$-methyltetrahydromethanopterin coenzyme-M methyltransferase from *Methanobacterium thermoautotrophicum*. *Eur. J. Biochem.* **213,** 537–545
4. Ellermann, J., Hedderich, R., Bocher, R., and Thauer, R. K. (1988) The final step in methane formation—investigations with highly purified methyl-CoM reductase (component C) from *Methanobacterium thermoautotrophicum* (strain Marburg). *Eur. J. Biochem.* **172,** 669–677
5. Setzke, E., Hedderich, R., Heiden, S., and Thauer, R. K. (1994) $H_2$-Heterodisulfide oxidoreductase complex from *Methanobacterium thermoautotrophicum*—composition and properties. *Eur. J. Biochem.* **220,** 139–148
6. Coskun, U., Chaban, Y. L., Lingl, A., Muller, V., Keegstra, W., Boekema, E. J., and Gruber, G. (2004) Structure and subunit arrangement of the A-type ATP synthase complex from the archaeon *Methanococcus jannaschii* visualized by electron microscopy. *J. Biol. Chem.* **279,** 38644–38648
7. Lange, S., and Fuchs, G. (1987) Autotrophic synthesis of activated acetic acid from $CO_2$ in *Methanobacterium thermoautotrophicum*—synthesis from tetrahydromethanopterin-bound C-1 units and carbon monoxide. *Eur. J. Biochem.* **163,** 147–154
8. Bonacker, L. G., Baudner, S., and Thauer, R. K. (1992) Differential expression of the 2 methyl-coenzyme M-reductases in *Methanobacterium thermoautotrophicum* as determined immunochemically via isoenzyme-specific antisera. *Eur. J. Biochem.* **206,** 87–92
9. Wackett, L. P., Hartwieg, E. A., King, J. A., Ormejohnson, W. H., and Walsh, C. T. (1987) Electron-microscopy of nickel-containing methanogenic enzymes—methyl reductase and $F_{420}$-reducing hydrogenase. *J. Bacteriol.* **169,** 718–727
10. Mayer, F., Rohde, M., Salzmann, M., Jussofie, A., and Gottschalk, G. (1988) The methanoreductosome—a high-molecular-weight enzyme complex in the methanogenic bacterium strain Go1 that contains components of the methylreductase system. *J. Bacteriol.* **170,** 1438–1444
11. Camacho-Carvajal, M. M., Wollscheid, B., Aebersold, R., Steimle, V., and Schamel, W. W. A. (2004) Two-dimensional blue native/SDS gel electrophoresis of multi-protein complexes from whole cellular lysates. A proteomics approach. *Mol. Cell. Proteomics* **3,** 176–182
12. Brookes, P. S., Pinner, A., Ramachandran, A., Coward, L., Barnes, S., Kim, H., and Darley-Usmar, V. M. (2002) High throughput two-dimensional blue-native electrophoresis: a tool for functional proteomics of mitochondria and signaling complexes. *Proteomics* **2,** 969–977
13. Nijtmans, L. G. J., Henderson, N. S., and Holt, I. J. (2002) Blue native electrophoresis to study mitochondrial and other protein complexes. *Methods* **26,** 327–334
14. Evguenieva-Hackenberg, E., Walter, P., Hochleitner, E., Lottspeich, F., and Klug, G. (2003) An exosome-like complex in *Sulfolobus solfataricus*. *EMBO Rep.* **4,** 889–893
15. Pennings, J. L. A., Vermeij, P., de Poorter, L. M. I., Keltjens, J. T., and Vogels, G. D. (2000) Adaptation of methane formation and enzyme contents during growth of *Methanobacterium thermoautotrophicum*

(strain Delta H) in a fed-batch fermentor. *Antonie Leeuwenhoek* **77,** 281–291
16. Staros, J. V., Wright, R. W., and Swingle, D. M. (1986) Enhancement by N-hydroxysulfosuccinimide of water-soluble carbodiimide-mediated coupling reactions. *Anal. Biochem.* **156,** 220–222
17. Schägger, H., de Coo, R., Bauer, M. F., Hofmann, S., Godinot, C., and Brandt, U. (2004) Significance of respirasomes for the assembly/stability of human respiratory chain complex I. *J. Biol. Chem.* **279,** 36349–36353
18. Arnold, I., Pfeiffer, K., Neupert, W., Stuart, R. A., and Schägger, H. (1998) Yeast mitochondrial F1F0-ATP synthase exists as a dimer: identification of three dimer-specific subunits. *EMBO J.* **17,** 7170–7178
19. Schägger, H., and von Jagow, G. (1987) Tricine sodium dodecyl-sulfate polyacrylamide-gel electrophoresis for the separation of proteins in the range from 1-kDa to 100-kDa. *Anal. Biochem.* **166,** 368–379
20. Candiano, G., Bruschi, M., Musante, L., Santucci, L., Ghiggeri, G. M., Carnemolla, B., Orecchia, P., Zardi, L., and Righetti, P. G. (2004) Blue silver: a very sensitive colloidal Coomassie G-250 staining for proteome analysis. *Electrophoresis* **25,** 1327–1333
21. Shevchenko, A., Jensen, O. N., Podtelejnikov, A. V., Sagliocco, F., Wilm, M., Vorm, O., Mortensen, P., Shevchenko, A., Boucherie, H., and Mann, M. (1996) Linking genome and proteome by mass spectrometry: large-scale identification of yeast proteins from two dimensional gels. *Proc. Natl. Acad. Sci. U. S. A.* **93,** 14440–14445
22. Bateman, A., Coin, L., Durbin, R., Finn, R. D., Hollich, V., Griffiths-Jones, S., Khanna, A., Marshall, M., Moxon, S., Sonnhammer, E. L. L., Studholme, D. J., Yeats, C., and Eddy, S. R. (2004) The Pfam protein families database. *Nucleic Acids Res.* **32,** D138–D141
23. Tatusova, T. A., and Madden, T. L. (1999) BLAST 2 SEQUENCES, a new tool for comparing protein and nucleotide sequences. *FEMS Microbiol. Lett.* **174,** 247–250
24. Riley, M. L., Schmidt, T., Wagner, C., Mewes, H. W., and Frishman, D. (2005) The PEDANT genome database in 2005. *Nucleic Acids Res.* **33,** D308–D310
25. Smith, D. R., DoucetteStamm, L. A., Deloughery, C., Lee, H. M., Dubois, J., Aldredge, T., Bashirzadeh, R., Blakely, D., Cook, R., Gilbert, K., Harrison, D., Hoang, L., Keagle, P., Lumm, W., Pothier, B., Qiu, D. Y., Spadafora, R., Vicaire, R., Wang, Y., Wierzbowski, J., Gibson, R., Jiwani, N., Caruso, A., Bush, D., Safer, H., Patwell, D., Prabhakar, S., McDougall, S., Shimer, G., Goyal, A., Pietrokovski, S., Church, G. M., Daniels, C. J., Mao, J. I., Rice, P., Nolling, J., and Reeve, J. N. (1997) Complete genome sequence of *Methanobacterium thermoautotrophicum* Delta H: functional analysis and comparative genomics. *J. Bacteriol.* **179,** 7135–7155
26. Brommelstroet, B. W. T., Hensgens, C. M. H., Keltjens, J. T., Vanderdrift, C., and Vogels, G. D. (1991) Purification and characterization of coenzyme-$F_{420}$-dependent 5,10-methylenetetrahydromethanopterin dehydrogenase from *Methanobacterium thermoautotrophicum* strain delta-H. *Biochim. Biophys. Acta* **1073,** 77–84
27. Wasserfallen, A., Huber, K., and Leisinger, T. (1995) Purification and structural characterization of a flavoprotein induced by iron limitation in *Methanobacterium thermoautotrophicum* Marburg. *J. Bacteriol.* **177,** 2436–2441
28. Eberhardt, S., Korn, S., Lottspeich, F., and Bacher, A. (1997) Biosynthesis of riboflavin: an unusual riboflavin synthase of *Methanobacterium thermoautotrophicum*. *J. Bacteriol.* **179,** 2938–2943
29. Ladenstein, R., Meyer, B., Huber, R., Labischinski, H., Bartels, K., Bartunik, H. D., Bachmann, L., Ludwig, H. C., and Bacher, A. (1986) Heavy riboflavin synthase from *Bacillus subtilis*—particle dimensions, crystal packing and molecular symmetry. *J. Mol. Biol.* **187,** 87–100
30. Baldwin, S. A., Perham, R. N., and Stribling, D. (1978) Purification and characterization of class-II D-fructose 1,6-bisphosphate aldolase from *Escherichia coli* (Crookes strain). *Biochem. J.* **169,** 633–641
31. Breinig, S., Kervinen, J., Stith, L., Wasson, A. S., Fairman, R., Wlodawer, A., Zdanov, A., and Jaffe, E. K. (2003) Control of tetrapyrrole biosynthesis by alternate quaternary forms of porphobilinogen synthase. *Nat. Struct. Biol.* **10,** 757–763
32. Bertram, P. A., Schmitz, R. A., Linder, D., and Thauer, R. K. (1994) Tungstate can substitute for molybdate in sustaining growth of *Methanobacterium thermoautotrophicum*—identification and characterization of a tungsten isoenzyme of formylmethanofuran dehydrogenase. *Arch. Microbiol.* **161,** 220–228
33. Schmitz, R. A., Albracht, S. P. J., and Thauer, R. K. (1992) A molybdenum and a tungsten isoenzyme of formylmethanofuran dehydrogenase in the thermophilic archaeon *Methanobacterium wolfei*. *Eur. J. Biochem.* **209,** 1013–1018
34. Schmitz, R. A., Richter, M., Linder, D., and Thauer, R. K. (1992) A tungsten-containing active formylmethanofuran dehydrogenase in the thermophilic archaeon *Methanobacterium wolfei*. *Eur. J. Biochem.* **207,** 559–565
35. Stojanowic, A., Mander, G. J., Duin, E. C., and Hedderich, R. (2003) Physiological role of the $F_{420}$ non-reducing hydrogenase (Mvh) from *Methanothermobacter marburgensis*. *Arch. Microbiol.* **180,** 194–203
36. Fox, J. A., Livingston, D. J., Ormejohnson, W. H., and Walsh, C. T. (1987) 8-Hydroxy-5-deazaflavin-reducing hydrogenase from *Methanobacterium thermoautotrophicum*. 1. Purification and characterization. *Biochemistry* **26,** 4219–4227
37. Weber, T., and Bach, T. J. (1994) Conversion of acetyl-coenzyme-A into 3-hydroxy-3-methylglutaryl-coenzyme-A in radish seedlings—evidence of a single monomeric protein catalyzing a Fe-II/quinone-stimulated double condensation reaction. *Biochim. Biophys. Acta* **1211,** 85–96
38. Nachin, L., Loiseau, L., Expert, D., and Barras, F. (2003) SufC: an unorthodox cytoplasmic ABC/ATPase required for [Fe-S] biogenesis under oxidative stress. *EMBO J.* **22,** 427–437
39. Rangachari, K., Davis, C. T., Eccleston, J. F., Hirst, E. M. A., Saldanha, J. W., Strath, M., and Wilson, R. J. M. (2002) SufC hydrolyzes ATP and interacts with SufB from *Thermotoga maritima*. *FEBS Lett.* **514,** 225–228
40. Koonin, E. V., Wolf, Y. I., and Aravind, L. (2001) Prediction of the archaeal exosome and its connections with the proteasome and the translation and transcription machineries by a comparative-genomic approach. *Genome Res.* **11,** 240–252
41. Maupin-Furlow, J. A., Gil, M. A., Karadzic, I. M., Kirkland, P. A., and Reuter, C. J. (2004) Proteasomes: perspectives from the Archaea. *Front. Biosci.* **9,** 1743–1758
42. Benaroudj, N., and Goldberg, A. L. (2000) PAN, the proteasome-activating nucleotidase from archaebacteria, is a protein-unfolding molecular chaperone. *Nat. Cell Biol.* **2,** 833–839
43. Wilson, H. L., Ou, M. S., Aldrich, H. C., and Maupin-Furlow, J. (2000) Biochemical and physical properties of the *Methanococcus jannaschii* 20S proteasome and PAN, a homolog of the ATPase (Rpt) subunits of the eucaryal 26S proteasome. *J. Bacteriol.* **182,** 1680–1692
44. Zwickl, P., Ng, D., Woo, K. M., Klenk, H. P., and Goldberg, A. L. (1999) An archaebacterial ATPase, homologous to ATPases in the eukaryotic 26 S proteasome, activates protein breakdown by 20 S proteasomes. *J. Biol. Chem.* **274,** 26008–26014
45. van Hoof, A., and Parker, R. (1999) The exosome: a proteasome for RNA? *Cell* **99,** 347–350
46. Lykke-Andersen, J., and Garrett, R. A. (1997) RNA-protein interactions of an archaeal homotetrameric splicing endoribonuclease with an exceptional evolutionary history. *EMBO J.* **16,** 6290–6300
47. Lilley, K. S., Razzaq, A., and Dupree, P. (2002) Two-dimensional gel electrophoresis: recent advances in sample preparation, detection and quantitation. *Curr. Opin. Chem. Biol.* **6,** 46–50
48. Rexroth, S., Meyer Zu Tittingdorf, J. M., Schwassmann, H. J., Krause, F., Seelert, H., and Dencher, N. A. (2004) Dimeric $H^+$-ATP synthase in the chloroplast of *Chlamydomonas reinhardtii*. *Biochim. Biophys. Acta* **1658,** 202–211
49. Schagger, H. (2002) Respiratory chain supercomplexes of mitochondria and bacteria. *Biochim. Biophys. Acta* **1555,** 154–159